Article

Quantum Chemical Studies on the Adsorption of Hexachlorobenzene, Decachlorobiphenyl, Benzene, and Biphenyl by BN-Doped Graphene and C-Doped Hexagonal Boron Nitride Modified with β-Cyclodextrin

Chien-Lin Lee, Tai-Chao Chang and Chia Ming Chang *

Environmental Molecular and Electromagnetic Physics (EMEP) Laboratory, Department of Soil and Environmental Sciences, National Chung Hsing University, Taichung 40227, Taiwan
* Correspondence: abinitio@dragon.nchu.edu.tw

Abstract: In this study, the adsorption of aromatic organic pollutants such as hexachlorobenzene, decachlorobiphenyl, benzene, and biphenyl by 2D nanomaterials was investigated using quantum chemical methods. The calculation results include reaction enthalpies, non-covalent intermolecular and intramolecular interactions, optimized structures, hydrogen bonds, and molecular electrostatic potentials. Fukui's FMO electrophile sensitivity is used to predict the most reactive positions on the chemical species for both nucleophilic and electrophilic roles. The results of hard–soft acid-base reactivity descriptors show that the electronic structures of BN-doped graphene and C-doped hexagonal boron nitride depend on the degree of doping and the modification of β-cyclodextrin. C doping helps to significantly improve the conductivity of h-BN, and β-cyclodextrin enhances the binding stability of aromatic organic pollutants. Hydrogen bonding between β-cyclodextrin and chlorine-substituted compounds can enhance non-covalent interactions. In particular, the high adsorption capacity and electron transfer capacity of decachlorobiphenyl laid the foundation for the development of new sensors.

1. Introduction

Cyclodextrin is series of cyclic oligosaccharides produced through glucotransferase by Bacillus, with multiple glucopyranose molecules composed of 1,4-glycosidic bonds in a cone-shaped cylindrical structure. The inner cavity of cyclodextrin is hydrophobic, while the outer cavity is hydrophilic. When the quantity of glucopyranose monomers is seven, it is called β-cyclodextrin (BCD), which has the inclusion mechanism [1] and characteristics of a moderate size for encapsulated molecules with a high stability [2], non-toxicity, high availability, and a low cost [3], making it the best choice for complexes that it enables interactions with organic or inorganic molecules [4–6]. Actually, the wide applications of surface BCD-functionalized substrates as a host–guest chemistry system in drug delivery, textiles, foods, chiral recognition, electrochemical sensing, and pollutant removal were summarized [7,8].

Sometimes β-cyclodextrin still faces the limitation of catalytic activity, and many researchers would modify the matrix to expand the scope of the applications [9]. Permethylated cyclodextrins or heptakis(2,6-di-*O*-methyl)-β-cyclodextrin (DIMEB) showed a more remarkable reduction in the volatility of fenitrothion to protect the insecticide molecule from a nucleophilic attack by the hydroxide ion [10,11]. Amidoxime-functionalized carboxymethyl β-cyclodextrin/graphene aerogel (GDC) for uranium extraction and crosslink cyclodextrin with epichlorohydrin for absorbing pesticides via CD inclusion, loading into swelling water, and physical adsorption were developed [12,13].

Chemical dyes with lots of benzene ring structures are colorful, but there are fatal risks. Consequently, much attention should be paid before discharge that several conventional technologies have been proposed for the treatment of dyes from wastewater such as liquid extraction, membrane filtration, and adsorption. Recently, researches have pointed out that magnetic β-cyclodextrin–chitosan/graphene oxide materials (MCCG) were fabricated as excellent adsorbents for bisphenol A (BPA) elimination through a facile chemical route [14]. Acid fuchsin and Rhodamine 6G could be effectively removed from their solutions by the magnetic GO-β-CD hybrid [15]. These principles are mainly benefiting from the surface properties of graphene oxide, the hydrophobicity of β-cyclodextrin, and magnetic functionalization [16,17]. Apart from that, it was found that anti-corrosion and inert performance are two of the most important roles for avoiding materials being destroyed by exterior factors. The observations of cerium acetylacetonate-loaded beta-cyclodextrin/graphene oxide (β-CD-CeA-MGO) derived from FE-SEM, EDS, and mapping investigations confirmed the formation of anti-corrosive film [18]. The corrosion protection performance and reduction in the electrolyte/ion diffusion was improved, assigning to β-CD-ZnA-MGO nano-filler in the epoxy resin matrix [19].

Graphene and hexagonal boron nitride belong to hexagonal system with a two-dimensional plane, and the former is arranged by sp^2 hybridized carbon atoms, whereas it is arranged by B atoms and N atoms for h-BN. In spite of the good optical, thermal, magnetic, and electronic performance of graphene, mechanical stability is requested when using it on any sphere. Hexagonal boron nitride as a substrate has been proved to solve this problem. For instance, a zero-band gap has hindered the construction of graphene-based devices. Then, the isoelectronic co-doping of B and N atoms, namely 2D h-BN, which could be formed to achieve the goal of regulating and maintaining graphene's geometrical and electrical properties [20].

The preparation of nanomaterials is not necessarily applicable to all conditions. Non-covalent and covalent functionalization can promote physicochemical properties for different targets [21]. Cyclodextrins with functionalized carbon nanotubes is possible for efficiently adsorbing p-nitrophenol compared to activated carbon [22]. In the field of persistent toxic substances (PTS), polychlorinated biphenyl (PCB) was determined by β-CD/CNTs/GCE [23]. Carbon nanotubes (CNTs)/β-cyclodextrin (β-CD) nanocomposite reinforcing hollow fiber (HF) was developed and exhibited an outstanding adsorption capacity, molecular recognition, sample clean-up effect, and pesticide residue analysis [24]. The β-CD/MWCNT-modified glassy carbon electrode showed a great response to the MCPA detection system, with a high sensitivity, stability, and lifetime [25]. β-cyclodextrin/graphene oxide gaining higher status results from the structure with a large porosity ratio to provide an exceptional adsorption capability, with more hydroxyl and carboxyl groups on the surface to improve its hydrophilicity. Accordingly, the achievements for applicability and diversity are limitless [26–31]. It is clear that adsorbents functionalized with cyclodextrins are a broad research field. On the other hand, it also motivates us to meet actual requirements and should focus on how to obtain the development to be widespread in the coming years.

Aromatic organic pollutants, which are insoluble in water and easily soluble in organic solvents, have a wide-application, including in agricultural drugs, industrial synthesis, and so on. Once they enter the ecosystem by the grasshopper effect, they will be harmful to the nerves, reproduction, and immune systems with biomagnification and bioaccumulation that might also cause cancer in severe cases. They have become a topic of international concern, e.g., hexachlorobenzene and decachlorobiphenyl, which have been listed as persistent organic pollutants (POPs), banned globally in the Stockholm Convention.

Both N-doped graphene and B-doped graphene has been used as chemical sensors for biomolecules due to the increase in the electronic density of states near the Fermi level [32,33]. Boron–carbon–nitride may act as a candidate for sensing applications with a superior binding strength to graphene and boron nitride-based materials [34]. Previous studies provided useful guidance for the gas sensing applications of pristine and amine-functionalized BNNTs to detect toxic gases at room temperature [35]. The encapsulation of the anti-cancer docetaxel drug (DTX) into BNNTs was studied by molecular dynamics

simulations in aqueous solution and EtOH co-solvent [36]. Previous literature based on density functional theory (DFT) and the semiempirical method PM7 analyzed the adsorption process of pollutant gases at different positions of BNNTs [37]. The adsorption distance and energy, charge transfer, and density of the states have been discussed based on the DFT method. Combined with the desorption time, Rh-BNNTs are theoretically predicted to have a potential as SO_2 gas sensor materials [38]. In order to address the challenges of improving the therapeutic efficiency, the bioavailability and reducing adverse side effects at the molecular level, the acid-functionalized CNTs with benserazide as a Levodopa nanodrug carrier complex, was calculated [39]. The anti-cancer molecule crizotinib (CZT) on the surface of CNTs and BNNTs was investigated using DFT and COSMO-RS. Simultaneously, compute quantum molecular descriptors (QMDs) accounted for drug–carrier interaction mechanisms and adsorption energies [40]. The results of the DFT calculations showed that the electronic properties of Pd/CNT changed significantly after CH_2O was adsorbed [41]. Studying the adsorption and encapsulation of the chemotherapeutic drug lomustine in CNTs by a DFT calculation has become an effective choice for designing drug carriers [42]. Applying L-leucine amino acid to Pd-loaded CNTs and reactive functional groups can combine hydrogen bonding, hydrophobic interactions, and Van der Waals forces with the protein surface during detection [43].

Thus, β-cyclodextrin as a molecular receptor and doped nanosheets as an enhancer of electron transfer are our concepts of designing electrochemical sensors. The objective of the work is to design a β-cyclodextrin-decorated nano-level biosensor to explore the selectivity of detecting aromatic organic pollutants and to realize the effect of doping and modifying with β-cyclodextrin.

2. Computational Details

BN-doped graphene (CC_BN) and C-doped hexagonal boron nitride (h-BN_CC) nanosheets terminated by hydrogen atoms along the edge are modeled with *Nanotube Modeler* software (JCrystalSoft, 2018) to generate the XYZ coordinates. Two and ten hexagonal doped islands are, respectively, named for serial number 1 and 2. The molecular structures of investigated aromatic organic pollutants, including hexachlorobenzene (cb), decachlorobiphenyl (pcb), benzene (b), and biphenyl (bp), are loaded from PubChem. The β-cyclodextrin molecule is downloaded from the Cambridge Structural Database (CSD) in the Cambridge Crystallographic Data Centre with the Entry: BCDEXD03. The ratio of β-cyclodextrin and pollutant molecule present 1:1 host–guest stoichiometry.

CC_BN and h-BN_CC with and without the functionalization of β-cyclodextrin on the doped site via the strategy of adsorption are calculated by the PM7 [44] level in MOPAC 2016, which is available from http://openmopac.net (accessed on 14 June 2021) [45,46]. The geometries of all the systems are fully optimized using tight optimization criteria with a gradient threshold of 4.2×10^{-4} kJ mol^{-1} Å^{-1}. The calculated results are illustrated by the MoCalc 2012 software to study the optimized structure, hydrogen bonding, and molecular electrostatic potential. MoCalc 2012 is also used to show non-covalent intermolecular and intramolecular interactions (NCI) [47,48] with colorful and continuous surfaces. Fukui's FMO electrophilic susceptibilities for predicting the most reactive position on chemical species are performed to realize the role of nucleophilicity (HOMO) and electrophilicity (LUMO), which are concluded in the previous literature [49].

3. Results and Discussions

3.1. Non-Covalent Interaction (NCI)

The color between carbon doping of hexagonal boron nitride and β-cyclodextrin is mainly composed of blue–green and yellow. Among them, the hydroxyl group on C6 of the β-cyclodextrin has a primary force of an electrostatic interaction. Both benzene and hexachlorobenzene with β-cyclodextrin all appear sporadic green. Even though the dipole moments of the two compounds above are zero, hexachlorobenzene bonds with

high-electronegative chlorine atoms, which can have more polarity with the surrounding functional groups, so the color distribution is denser.

The increase in the distribution range of other colors and blue areas shows that the biphenyl morphology with an increasing guest molecular size forms more and stronger dispersive interactions than a single benzene ring structure [50]. One aromatic ring of biphenyl and decachlorobiphenyl locating near the adsorbent is wrapped in yellow, blue–green. Biphenyl has a weaker interaction with β-cyclodextrin compared with decachlorobiphenyl and obvious differences are performed especially between the chlorine atoms of decachlorobiphenyl and the hydrogen atoms of β-cyclodextrin. The inner cavity of β-cyclodextrin due to the shielding effect of the C-H bond forms host–guest inclusion complexes for these aromatic congeners through dominant hydrophobic, Van der Waals interactions [51–53].

In addition, Figure 1A,C show that there are hardly non-covalent interactions covered at the center of C-doping; otherwise, the abundance of delocalized π-electrons in the C-doped site of h-BN make a large area of dark blue demonstrated together with decachlorobiphenyl from Figure 1B. A previous study indicated the high adsorption of polychlorinated biphenyls [54]. Therefore, it can be inferred that the graphene-like structure is favorable for the adsorption of decachlorobiphenyl via stronger π-π stacking [55,56]. In addition, there are Van der Waals, π-π interactions and the Lewis acid-base interactions between BN-based materials and adsorbate [57,58].
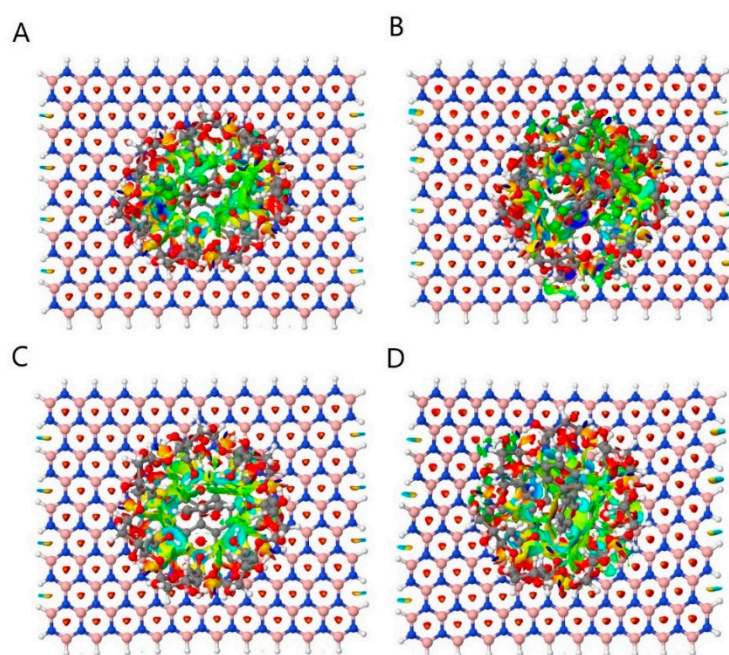

Figure 1. Non-covalent interaction between (**A**) hexachlorobenzene (cb), (**B**) decachlorobiphenyl (pcb), (**C**) benzene (b), and (**D**) biphenyl (bp) and carbon-doped hexagonal boron nitride (h-BN-CC2) decorated with beta-cyclodextrin (BCD).

3.2. Equilibrium Structure and Reaction Enthalpy

Hexachlorobenzene and decachlorobiphenyl are all Cl substitution; however, the carbon on benzene ring structure lacks the attractiveness of the electrons and the chlorine atoms themselves are not easy to assume σ-hole state to form halogen bonds. After the addition and modification of β-cyclodextrin, a large number of hydroxyl groups help the adsorption function. Hydrogen bonds which would keep ring-shaped-like geometric complexes stabilized are shown as the figure; because of the characteristics of high electronegativity, the chlorine atoms of hexachlorobenzene and decachlorobiphenyl play important hydrogen bond acceptors [59]. There are four hydrogen bonds formed between hexachlorobenzene and β-cyclodextrin with their average bond length of 2.94 Å, and there

are as many as six hydrogen bonds on decachlorobiphenyl where the average bond length is about 2.96 Å.

CC_BN2 adsorbing β-cyclodextrin release the most adsorption energy, followed by h-BN_CC2, which can form stable structures. From the adsorption status of CC_BN_BCD, it can be seen that the adsorption energy for hexachlorobenzene and decachlorobiphenyl is more than the other two pollutants that it is found to be correlated with the hydrophobicity of the pollutants [60]. When CC_BN1_BCD is converted to CC_BN2_BCD, the adsorption energy of chlorine-containing compounds is reduced, whereas benzene and biphenyl show an increase. Although the adsorption capacity of the latter two is improved, they are still inferior to hexachlorobenzene and decachlorobiphenyl, which are related to the electrostatic potential of the partial charge of the chlorine atoms and the BN-doped site. As for h-BN_CC_BCD, the one with the largest adsorption energy is decachlorobiphenyl, and benzene is the smallest. In particular, decachlorobiphenyl is immobilized by h-BN_CC2_BCD the most in Table 1 through the strategy of adsorption.

Table 1. Reaction enthalpy (ΔH_f in kcal/mol) of hexachlorobenzene (cb), decachlorobiphenyl (pcb), benzene (b), and biphenyl (bp) adsorbed by the nano-systems of BN-doped graphene (CC-BN1 and CC-BN2) and carbon-doped hexagonal boron nitride (h-BN-CC1 and h-BN-CC2) decorated with beta-cyclodextrin (BCD).

			Reaction Enthalpy (ΔH_f) (kcal/mol)
CC_BN1	+BCD	→CC_BN1_BCD	−72.1674
CC_BN2	+BCD	→CC_BN2_BCD	−92.0323
h-BN_CC1	+BCD	→h-BN_CC1_BCD	−76.3327
h-BN_CC2	+BCD	→h-BN_CC2_BCD	−77.2604
CC_BN1_BCD	+cb	→CC_BN1_BCD_cb	−60.9593
CC_BN1_BCD	+pcb	→CC_BN1_BCD_pcb	−94.6094
CC_BN1_BCD	+b	→CC_BN1_BCD_b	−24.2197
CC_BN1_BCD	+bp	→CC_BN1_BCD_bp	−22.9383
CC_BN2_BCD	+cb	→CC_BN2_BCD_cb	−52.5011
CC_BN2_BCD	+pcb	→CC_BN2_BCD_pcb	−88.8037
CC_BN2_BCD	+b	→CC_BN2_BCD_b	−28.7710
CC_BN2_BCD	+bp	→CC_BN2_BCD_bp	−41.4766
h-BN_CC1_BCD	+cb	→h-BN_CC1_BCD_cb	−50.0348
h-BN_CC1_BCD	+pcb	→h-BN_CC1_BCD_pcb	−97.4077
h-BN_CC1_BCD	+b	→h-BN_CC1_BCD_b	−31.9365
h-BN_CC1_BCD	+bp	→h-BN_CC1_BCD_bp	−46.1465
h-BN_CC2_BCD	+cb	→h-BN_CC2_BCD_cb	−45.7307
h-BN_CC2_BCD	+pcb	→h-BN_CC2_BCD_pcb	−110.203
h-BN_CC2_BCD	+b	→h-BN_CC2_BCD_b	−14.9105
h-BN_CC2_BCD	+bp	→h-BN_CC2_BCD_bp	−55.5254

As the number of C-doping increases, it is conducive to the adsorption capacity of biphenyl derivatives, while benzene and hexachlorobenzene weaken. Moreover, when h-BN_CC2_BCD adsorbs these four pollutants, the magnitude of the adsorption energy coincides with the color distribution in Figure 1, indicating that the non-covalent interaction is the key to this spontaneous and physical adsorption. Regardless of the adsorbent, the reaction enthalpy produced by decachlorobiphenyl is much greater than that of hexachlorobenzene. According to Figure 2, the difference in the energy comes from the number of hydrogen bonds. In the same way, it can be proved that benzene and biphenyl are not easy to form hydrogen bonds with β-cyclodextrin; thus, the adsorption value is generally low.
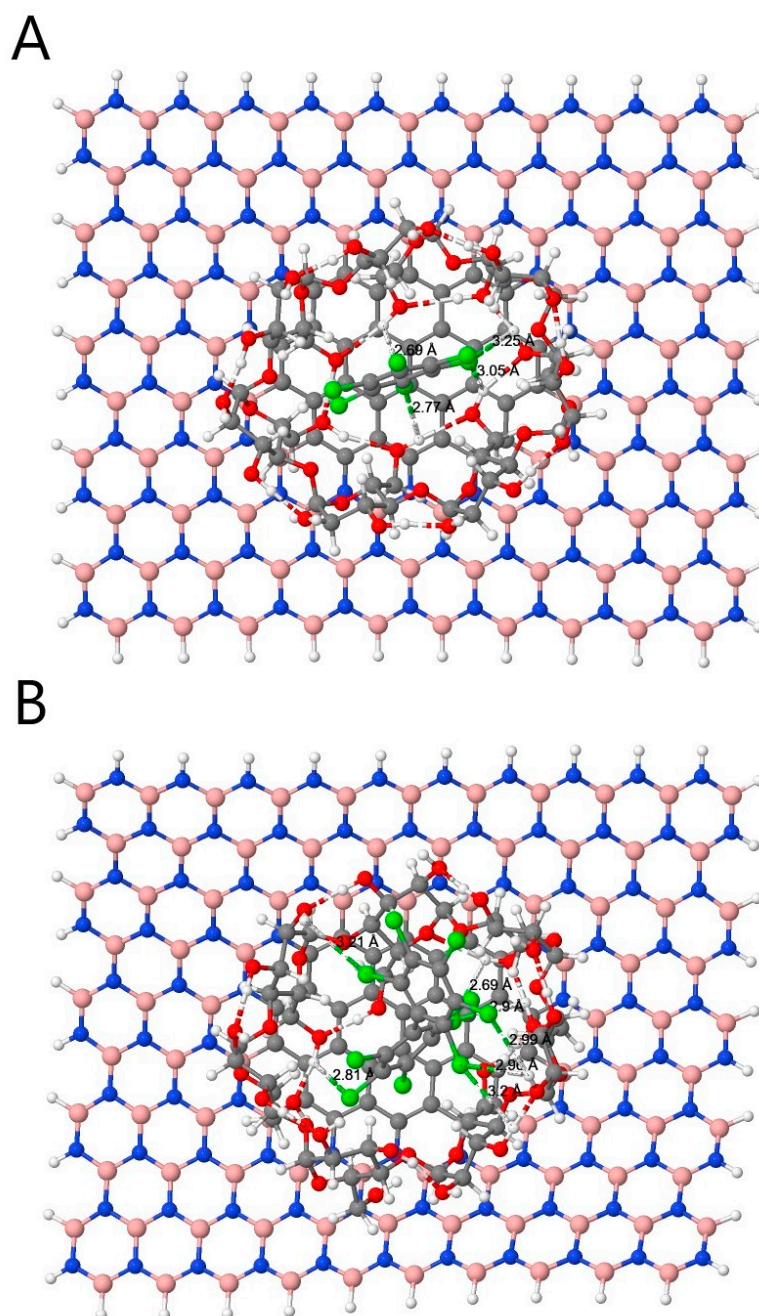
Figure 2. Equilibrium structures of (**A**) hexachlorobenzene (cb) and (**B**) decachlorobiphenyl (pcb) adsorbed on carbon-doped hexagonal boron nitride (h-BN-CC2) decorated with beta-cyclodextrin (BCD).

3.3. Molecular Electrostatic Potential

On hexachlorobenzene and decachlorobiphenyl, the inside of the benzene ring is light yellow, because the benzene ring is connected to a chlorine atom and the chlorine atom with a high electronegativity will attract electrons (Figure 3A,B). The color of the electrostatic potential map on benzene is red, yellow, and green from the inside to the outside. The outside of the benzene ring is mainly neutral, while the hydrogen atom is light blue with a weak positive charge. The color of the electrostatic potential on biphenyl is similar to the benzene ring, but only yellow in the benzene ring (Figure 3C,D).
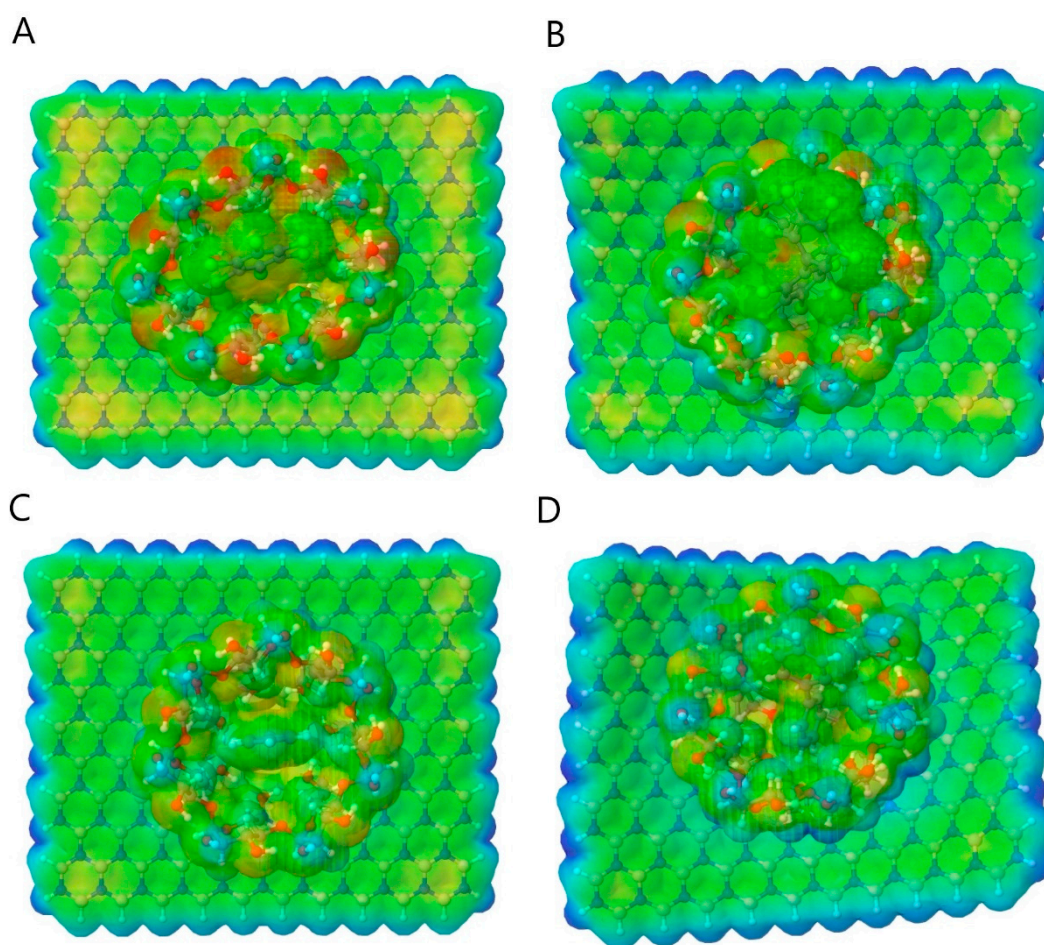
Figure 3. Electrostatic potential of (**A**) hexachlorobenzene (cb), (**B**) decachlorobiphenyl (pcb), (**C**) benzene (b), and (**D**) biphenyl (bp) adsorbed on carbon-doped hexagonal boron nitride (h-BN-CC2) decorated with beta-cyclodextrin (BCD).

The adsorption site of h-BN is mainly orange and negatively charged. The entire cyclodextrin is mainly green, which means that most of it is electrically neutral, and the electrostatic force is evenly distributed, which also means that the polarity is not obvious. The adsorption is relatively less affected by the electrostatic force, and the charge difference of each part is not large and tends to be neutral. However, on the oxygen, it is orange–red with a negative charge, while the outer hydrogen atom is light blue with a positive charge, which is consistent with the hydrophobicity of the inner side of the cyclodextrin and the hydrophilicity of the outer side in the literature. What is more special is the chlorine atom. According to its electronegativity, the chlorine atom has a strong attraction to the electrons and should appear reddish-yellow. However, due to the influence of its atomic radius, the electrostatic potential of the entire atom is not obvious and it still belongs to the electron-rich region.

3.4. Frontier Molecular Orbital Electrophilic Susceptibility

The results of the frontier molecular orbital for the h-BN nanosheet (excluding C-doped zone) are very similar, and nitrogen prefers to attract electrons than boron; red electrophilic positions are concentrated on the upper nanosheet moieties and located at N and the N-B bond. The molecular size of β-cyclodextrin is the same as that of the C-doped region, whose adsorption site is mainly yellow–green with a little red sprinkling, and the scope of the molecular orbital is expanded to carbon atoms and carbon–carbon bonds. Dark blue performed on the center near the pollutants means the most susceptibility to an electrophile attack.

Figure 4A,C,D represent the co-adsorption of hexachlorobenzene, benzene, biphenyl with β-cyclodextrin, respectively, and each of them exhibits an identical appearance. Only the aromatic ring of decachlorobiphenyl closed to h-BN_CC2 is densely covered with red (Figure 4B), which forms a strong electron donor-acceptor with the green orbital on a graphene-like island. It is better than the other compounds in terms of the efficiency of the electron transfer.
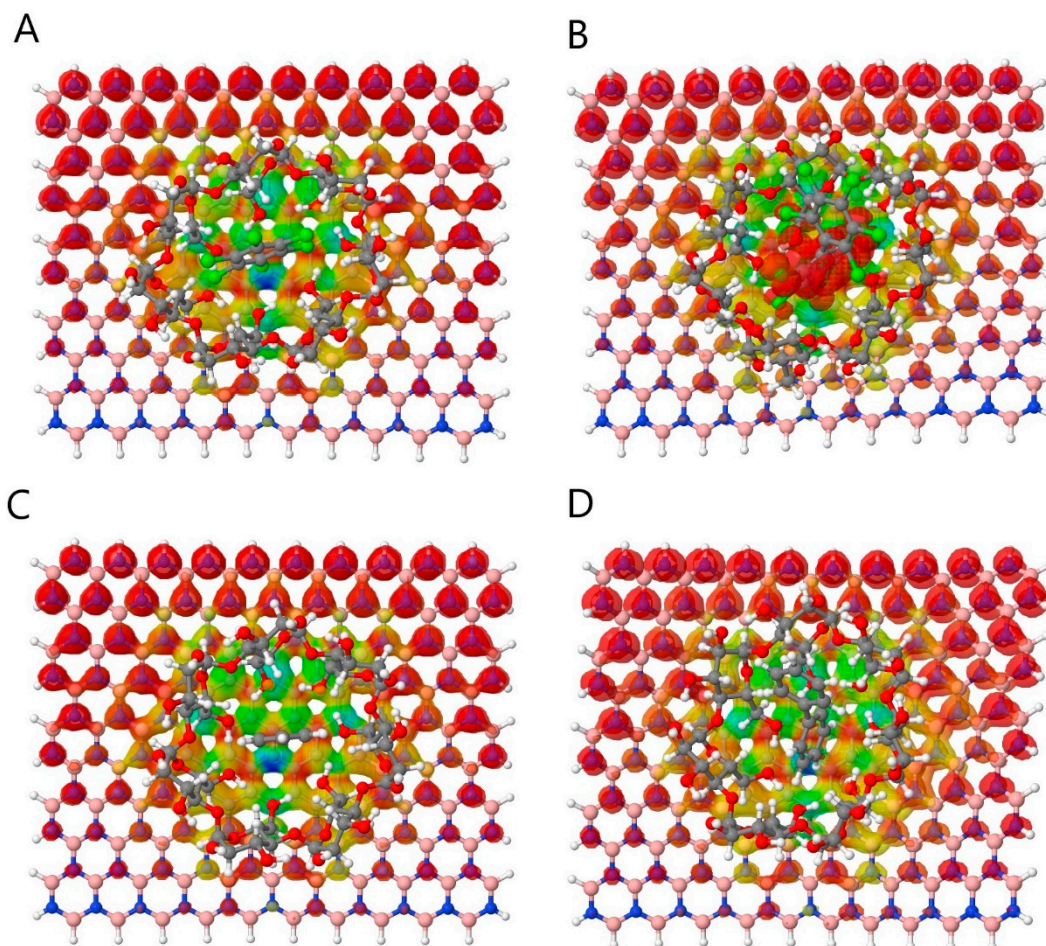

Figure 4. Frontier molecular orbital electrophilic susceptibility of (**A**) hexachlorobenzene (cb), (**B**) decachlorobiphenyl (pcb), (**C**) benzene (b), and (**D**) biphenyl (bp) adsorbed on carbon-doped hexagonal boron nitride (h-BN-CC2) decorated with beta-cyclodextrin (BCD).

3.5. Hard–Soft Acid-Base (HSAB) Reactivity Descriptor

All the descriptors in Table 2 are obtained from the calculations of the HOMO (the highest occupied molecular orbital) and LUMO (the lowest unoccupied molecular orbital) for every molecule. In terms of doping, the change in the ionization energy caused by C-doping is larger than that of BN-doping. As the number of C-doping increases, the ionization energy of the h-BN nanosheet decreases more significantly, and it also happens for decorated h-BN_CC by β-cyclodextrin. When β-cyclodextrin is adsorbed on the nanosheet, the ionization energy of CC_BN becomes larger, and that of h-BN_CC instead decreases.

According to Table 2, the electron affinity and electronegativity of h-BN_CC and h-BN_CC_BCD are less than CC_BN and CC_BN_BCD whether the substrate is decorated or not, especially as h-BN_CC2 all exhibits the lowest value of electronegativity with and without decoration, indicating that β-cyclodextrin helps h-BN to further reduce the attraction to electrons. The electronegativity of chlorine-containing compounds is indeed greater than that of benzene and biphenyl, especially decachlorobiphenyl with the largest value.

Table 2. The HSAB reactivity descriptors in the present study.

	GAP (eV)	I (eV)	A (eV)	χ (eV)	η (eV)	μ (eV)	S (eV^{-1})	ω (eV)
CC_BN1	2.796	6.418	3.622	5.020	1.398	−5.020	0.358	9.013
CC_BN2	2.736	6.343	3.607	4.975	1.368	−4.975	0.365	9.046
h-BN_CC1	5.477	7.396	1.919	4.658	2.739	−4.658	0.183	3.961
h-BN_CC2	4.957	6.964	2.007	4.486	2.479	−4.486	0.202	4.059
BCD	11.113	10.177	−0.936	4.621	5.557	−4.621	0.090	1.921
CC_BN1_BCD	2.788	6.463	3.675	5.069	1.394	−5.069	0.359	9.216
CC_BN2_BCD	2.727	6.388	3.661	5.025	1.364	−5.025	0.367	9.258
h-BN_CC1_BCD	5.351	7.320	1.969	4.645	2.676	−4.645	0.187	4.031
h-BN_CC2_BCD	4.842	6.890	2.048	4.469	2.421	−4.469	0.207	4.125
cb	8.542	10.180	1.638	5.909	4.271	−5.909	0.117	4.088
pcb	8.358	10.117	1.759	5.938	4.179	−5.938	0.120	4.219
b	10.060	9.824	−0.236	4.794	5.030	−4.794	0.099	2.285
bp	9.134	9.292	0.158	4.725	4.567	−4.725	0.109	2.444
CC_BN1_BCD_cb	2.792	6.478	3.686	5.082	1.396	−5.082	0.358	9.250
CC_BN1_BCD_pcb	2.741	6.441	3.700	5.071	1.371	−5.071	0.365	9.380
CC_BN1_BCD_b	2.789	6.467	3.678	5.073	1.395	−5.073	0.359	9.226
CC_BN1_BCD_bp	2.794	6.462	3.668	5.065	1.397	−5.065	0.358	9.182
CC_BN2_BCD_cb	2.720	6.390	3.670	5.030	1.360	−5.030	0.368	9.302
CC_BN2_BCD_pcb	2.805	6.407	3.602	5.005	1.403	−5.005	0.357	8.929
CC_BN2_BCD_b	2.743	6.387	3.644	5.016	1.372	−5.016	0.365	9.171
CC_BN2_BCD_bp	2.738	6.384	3.646	5.015	1.369	−5.015	0.365	9.186
h-BN_CC1_BCD_cb	5.365	7.345	1.980	4.663	2.683	−4.663	0.186	4.052
h-BN_CC1_BCD_pcb	5.428	7.409	1.981	4.695	2.714	−4.695	0.184	4.061
h-BN_CC1_BCD_b	5.375	7.343	1.968	4.656	2.688	−4.656	0.186	4.032
h-BN_CC1_BCD_bp	5.378	7.350	1.972	4.661	2.689	−4.661	0.186	4.040
h-BN_CC2_BCD_cb	4.833	6.911	2.078	4.495	2.417	−4.495	0.207	4.180
h-BN_CC2_BCD_pcb	4.949	7.001	2.052	4.527	2.475	−4.527	0.202	4.140
h-BN_CC2_BCD_b	4.810	6.871	2.061	4.466	2.405	−4.466	0.208	4.147
h-BN_CC2_BCD_bp	4.887	6.946	2.059	4.503	2.444	−4.503	0.205	4.148

μ is the chemical potential, which is described by electronegativity with an opposite sign. The greater the value of μ, the more likely it is to provide electrons to those with a lower chemical potential. Before the adsorption of β-cyclodextrin, once the number of dopes increases, the chemical potential can raise, and C-doping has a deeper impact on hexagonal boron nitride. As β-cyclodextrin is attached to the material, it continues to make the value of the chemical potential larger compared with the pristine h-BN_CC, but CC_BN has a consequence contrary to expectation. Combining the above description and Table 2, the μ value of h-BN_CC2_BCD reaches −4.469 eV, the maximum of all the materials. In view of the high chemical potential of h-BN_CC2_BCD, it drives to enhance the electron flow to pollutants, especially decachlorobiphenyl, as the difference in the chemical potential is quite large. Thereby, from the comparison of the chemical potential between h-BN_CC2/β-cyclodextrin and pollutants, the electron flow direction is exactly in line with Figure 4.

η is the chemical hardness. The greater the chemical hardness, the less likely to be polarized and the molecular structure is stable. S is the chemical softness, and its physical and chemical properties reflect opposite data and trends. Because the hydroxyl groups form intramolecular hydrogen bonds with each other, β-cyclodextrin has the highest stability. Although the decoration of β-cyclodextrin and doping cause a decrease in the chemical hardness, h-BN_CC is still more suitable to be a stable material than CC_BN. Next, lower polar h-BN_CC2_BCD is combined with decachlorobiphenyl, which possesses the least η value due to the steric-hindrance effect, resulting in high reaction enthalpy. As far as chemical hardness is concerned, decachlorobiphenyl adsorbed by h-BN_CC2_BCD to be the most stable complex provides a perfect support.

ω is the electrophilic index, which can be used as a basis for the degree of accepting electrons. CC_BN is far easier to accept electrons than h-BN_CC, which displays the potential of an electron transfer. The decoration of β-cyclodextrin makes the electrophilic index increase slightly, and the negligible change in the latter is merely less than 0.1 eV. Decachlorobiphenyl has the largest electrophilic index, which confirms the phenomenon of the benzene ring structure covered by the red molecular orbital function as in Figure 4.

The band gap is regarding the electron transition; if the addition of a molecule makes the change in the gap between orbitals enormous enough, the fabrication of the sensors is promising. For GAP in Table 2, the factor of the number of C-doping makes it decrease more than 0.5 eV, showing that the efficiency of the improvement in the conductivity is more excellent than that of BN-doping. Whether a nanosheet is combined with β-cyclodextrin, CC_BN has a better conductivity than h-BN_CC owing to the graphene as the base. However, it is undeniable that β-cyclodextrin is conducive to the reduction in the original GAP, and even the effect on h-BN_CC is more distinct (decrease by at least 0.1 eV). In fact, analyzing the GAP variation, these four nanomaterials have a good sensing ability of decachlorobiphenyl and the most extraordinary exhibition of h-BN_CC2_BCD is as high as 0.107 eV. If h-BN_CC2_BCD is utilized alone nowadays, the detection of biphenyl is great as well.

β-cyclodextrin-functionalized nanosheet composites show excellent electrochemical sensing, which is attributed to the synergistic effects that can simultaneously combine the properties of the individual constituent materials (the electrocatalytic properties from the carbon-doped site and supramolecular recognition from β-CD) [61,62]. By the way, previous study has presented that non-covalent functionalization by β-cyclodextrin has the potential to improve the graphene dispersibility in the solvent [63], that it is a kind of material which is easy to handle and cost-saving. To sum up, C-doping and β-cyclodextrin have successfully enhanced the conductivity of the h-BN_CC nanosheet to 4.842 eV herein. Furthermore, the performances of the adsorption mechanism and acceleration of the electron transfer are sufficient to prove that h-BN_CC2_BCD has a high sensitivity to decachlorobiphenyl through the method of adsorption in the environment and has a place in separating neutral decachlorobiphenyl from polluted water.

4. Conclusions

The degree of doping and modification of β-cyclodextrin has a significant impact on the electronic structure of 2D nanomaterials. This study found that C-doping is more effective than BN-doping in enhancing the conductivity. The β-cyclodextrin-modified C-doped h-BN forms a hydrophobic cavity, which provides a larger adsorption area for aromatic organic pollutants. Meanwhile, the hydrogen bonding between β-cyclodextrin and chlorine-substituted compounds can strengthen the non-covalent interaction. Therefore, h-BN_CC2_BCD has the highest adsorption capacity and sensitivity for the removal and detection of decachlorobiphenyl.

Author Contributions: Conceptualization, C.-L.L., T.-C.C. and C.M.C.; methodology, C.-L.L., T.-C.C. and C.M.C.; software, C.-L.L. and T.-C.C.; validation, C.M.C.; formal analysis, C.-L.L., T.-C.C. and C.M.C.; investigation, C.-L.L.; resources, C.M.C.; data curation, C.-L.L.; writing—original draft preparation, C.-L.L.; writing—review and editing, C.M.C.; visualization, C.-L.L., T.-C.C. and C.M.C.; supervision, C.M.C.; project administration, C.M.C.; funding acquisition, C.M.C. All authors have read and agreed to the published version of the manuscript.

Conflicts of Interest: The authors declare no conflict of interest.

References

1. Liu, P.; Zhang, D.; Zhan, J. Investigation on the inclusions of PCB52 with cyclodextrins by performing DFT calculations and molecular dynamics simulations. *J. Phys. Chem. A* **2010**, *114*, 13122–13128. [CrossRef] [PubMed]
2. Campos, E.V.R.; Proença, P.L.F.; Oliveira, J.L.; Melville, C.C.; Della Vechia, J.F.; de Andrade, D.J.; Fraceto, L.F. Chitosan nanoparticles functionalized with β-cyclodextrin: A promising carrier for botanical pesticides. *Sci. Rep.* **2018**, *8*, 2067. [CrossRef] [PubMed]
3. Alsbaiee, A.; Smith, B.J.; Xiao, L.; Ling, Y.; Helbling, D.E.; Dichtel, W.R. Rapid removal of organic micropollutants from water by a porous β-cyclodextrin polymer. *Nature* **2016**, *529*, 190–194. [CrossRef] [PubMed]
4. Sun, Z.-Y.; Shen, M.-X.; Yang, A.-W.; Liang, C.-Q.; Wang, N.; Cao, G.-P. Introduction of β-cyclodextrin into poly(aspartic acid) matrix for adsorption and time-release of ibuprofen. *Chem. Commun.* **2011**, *47*, 1072–1074. [CrossRef] [PubMed]
5. Jiang, Y.; Abukhadra, M.R.; Refay, N.M.; Sharaf, M.F.; El-Meligy, M.A.; Awwad, E.M. Synthesis of chitosan/MCM-48 and β-cyclodextrin/MCM-48 composites as bio-adsorbents for environmental removal of Cd^{2+} ions; kinetic and equilibrium studies. *React. Funct. Polym.* **2020**, *154*, 104675. [CrossRef]
6. Song, W.; Shao, D.; Lu, S.; Wang, X. Simultaneous removal of uranium and humic acid by cyclodextrin modified graphene oxide nanosheets. *Sci. China Chem.* **2014**, *57*, 1291–1299. [CrossRef]
7. Abd-Elhamid, A.I.; El-Aassar, M.R.; El Fawal, G.F.; Soliman, H.M.A. Fabrication of polyacrylonitrile/β-cyclodextrin/graphene oxide nanofibers composite as an efficient adsorbent for cationic dye. *Environ. Nanotechnol. Monit. Manag.* **2019**, *11*, 100207. [CrossRef]
8. Lee, J.-u.; Lee, S.-S.; Lee, S.; Oh, H.B. Noncovalent Complexes of Cyclodextrin with Small Organic Molecules: Applications and Insights into Host–Guest Interactions in the Gas Phase and Condensed Phase. *Molecules* **2020**, *25*, 4048. [CrossRef]
9. Shen, C.; Yang, X.; Wang, Y.; Zhou, J.; Chen, C. Complexation of capsaicin with β-cyclodextrins to improve pesticide formulations: Effect on aqueous solubility, dissolution rate, stability and soil adsorption. *J. Incl. Phenom. Macrocycl. Chem.* **2012**, *72*, 263–274. [CrossRef]
10. Cruickshank, D.; Rougier, N.M.; Vico, R.V.; Rossi, R.H.d.; Buján, E.I.; Bourne, S.A.; Caira, M.R. Solid-state structures and thermal properties of inclusion complexes of the organophosphate insecticide fenitrothion with permethylated cyclodextrins. *Carbohydr. Res.* **2010**, *345*, 141–147. [CrossRef]
11. Cruickshank, D.; Rougier, N.; Raquel, V.; Bourne, S.; Buján, E.; Caira, M.; de Rossi, R. Inclusion of the insecticide fenitrothion in dimethylated-β-cyclodextrin: Unusual guest disorder in the solid state and efficient retardation of the hydrolysis rate of the complexed guest in alkaline solution. *Beilstein J. Org. Chem.* **2013**, *9*, 106–117. [CrossRef] [PubMed]
12. Li, N.; Yang, L.; Wang, D.; Tang, C.; Deng, W.; Wang, Z. High-Capacity Amidoxime-Functionalized β-Cyclodextrin/Graphene Aerogel for Selective Uranium Capture. *Environ. Sci. Technol.* **2021**, *55*, 9181–9188. [CrossRef] [PubMed]
13. Liu, H.; Cai, X.; Wang, Y.; Chen, J. Adsorption mechanism-based screening of cyclodextrin polymers for adsorption and separation of pesticides from water. *Water Res.* **2011**, *45*, 3499–3511. [CrossRef]
14. Gupta, V.K.; Agarwal, S.; Sadegh, H.; Ali, G.A.M.; Bharti, A.K.; Hamdy Makhlouf, A.S. Facile route synthesis of novel graphene oxide-β-cyclodextrin nanocomposite and its application as adsorbent for removal of toxic bisphenol A from the aqueous phase. *J. Mol. Liq.* **2017**, *237*, 466–472. [CrossRef]
15. Liu, X.; Yan, L.; Yin, W.; Zhou, L.; Tian, G.; Shi, J.; Yang, Z.; Xiao, D.; Gu, Z.; Zhao, Y. A magnetic graphene hybrid functionalized with beta-cyclodextrins for fast and efficient removal of organic dyes. *J. Mater. Chem. A* **2014**, *2*, 12296–12303. [CrossRef]
16. Fan, L.; Luo, C.; Sun, M.; Qiu, H.; Li, X. Synthesis of magnetic β-cyclodextrin–chitosan/graphene oxide as nanoadsorbent and its application in dye adsorption and removal. *Colloids Surf. B Biointerfaces* **2013**, *103*, 601–607. [CrossRef]
17. Li, L.; Fan, L.; Duan, H.; Wang, X.; Luo, C. Magnetically separable functionalized graphene oxide decorated with magnetic cyclodextrin as an excellent adsorbent for dye removal. *RSC Adv.* **2014**, *4*, 37114–37121. [CrossRef]
18. Dehghani, A.; Bahlakeh, G.; Ramezanzadeh, B. Designing a novel targeted-release nano-container based on the silanized graphene oxide decorated with cerium acetylacetonate loaded beta-cyclodextrin (*β*-CD-CeA-MGO) for epoxy anti-corrosion coating. *Chem. Eng. J.* **2020**, *400*, 125860. [CrossRef]
19. Dehghani, A.; Bahlakeh, G.; Ramezanzadeh, B. Synthesis of a non-hazardous/smart anti-corrosion nano-carrier based on beta-cyclodextrin-zinc acetylacetonate inclusion complex decorated graphene oxide (*β*-CD-ZnA-MGO). *J. Hazard. Mater.* **2020**, *398*, 122962. [CrossRef]
20. Wang, J.; Ma, F.; Sun, M. Graphene, hexagonal boron nitride, and their heterostructures: Properties and applications. *RSC Adv.* **2017**, *7*, 16801–16822. [CrossRef]
21. Amieva, E.J.; Lópeš Barroso, J.; Martínez-Hernández, A.; Velasco-Santos, C. Graphene-based materials functionalization with natural polymeric biomolecules. *Recent Adv. Graphene Res.* **2016**, *1*, 257–298.
22. Salipira, K.; Mamba, B.; Krause, R.; Malefetse, T.; Durbach, S. Carbon nanotubes and cyclodextrin polymers for removing organic pollutants from water. *Environ. Chem. Lett.* **2007**, *5*, 13–17. [CrossRef]
23. Xie, F.; Yang, M.; Jiang, M.; Huang, X.-J.; Liu, W.-Q.; Xie, P.-H. Carbon-based nanomaterials—A promising electrochemical sensor toward persistent toxic substance. *TrAC Trends Anal. Chem.* **2019**, *119*, 115624. [CrossRef]
24. Ding, Y.; Song, X.; Chen, J. Analysis of Pesticide Residue in Tomatoes by Carbon Nanotubes/β-Cyclodextrin Nanocomposite Reinforced Hollow Fiber Coupled with HPLC. *J. Food Sci.* **2019**, *84*, 1651–1659. [CrossRef]

25. Rahemi, V.; Vandamme, J.; Garrido, J.; Borges, F.; Brett, C.; Garrido, E. Enhanced host–guest electrochemical recognition of herbicide MCPA using a β-cyclodextrin carbon nanotube sensor. *Talanta* **2012**, *99*, 288–293. [CrossRef]

26. Rathour, R.K.S.; Bhattacharya, J.; Mukherjee, A. β-Cyclodextrin conjugated graphene oxide: A regenerative adsorbent for cadmium and methylene blue. *J. Mol. Liq.* **2019**, *282*, 606–616. [CrossRef]

27. Wu, Y.; Zhao, Z.; Chen, M.; Jing, Z.; Qiu, F. β-Cyclodextrin–graphene oxide–diatomaceous earth material: Preparation and its application for adsorption of organic dye. *Mon. Chem.-Chem. Mon.* **2018**, *149*, 1367–1377. [CrossRef]

28. Yang, Z.; Liu, X.; Liu, X.; Wu, J.; Zhu, X.; Bai, Z.; Yu, Z. Preparation of β-cyclodextrin/graphene oxide and its adsorption properties for methylene blue. *Colloids Surf. B Biointerfaces* **2021**, *200*, 111605. [CrossRef]

29. Xu, W.; Li, X.; Wang, L.; Li, S.; Chu, S.; Wang, J.; Li, Y.; Hou, J.; Luo, Q.; Liu, J. Design of Cyclodextrin-Based Functional Systems for Biomedical Applications. *Front. Chem.* **2021**, *9*, 635507. [CrossRef]

30. Zheng, H.; Gao, Y.; Zhu, K.; Wang, Q.; Wakeel, M.; Wahid, A.; Alharbi, N.S.; Chen, C. Investigation of the adsorption mechanisms of Pb(II) and 1-naphthol by β-cyclodextrin modified graphene oxide nanosheets from aqueous solution. *J. Colloid Interface Sci.* **2018**, *530*, 154–162. [CrossRef]

31. Maciel, E.V.S.; Mejía-Carmona, K.; Jordan-Sinisterra, M.; da Silva, L.F.; Vargas Medina, D.A.; Lanças, F.M. The Current Role of Graphene-Based Nanomaterials in the Sample Preparation Arena. *Front. Chem.* **2020**, *8*, 664. [CrossRef]

32. Banerjee, A.N. Graphene and its derivatives as biomedical materials: Future prospects and challenges. *Interface Focus* **2018**, *8*, 20170056. [CrossRef] [PubMed]

33. Putri, L.K.; Ong, W.-J.; Chang, W.S.; Chai, S.-P. Heteroatom doped graphene in photocatalysis: A review. *Appl. Surf. Sci.* **2015**, *358*, 2–14. [CrossRef]

34. Mir, S.; Yadav, V.; Singh, J. Boron–Carbon–Nitride Sheet as a Novel Surface for Biological Applications: Insights from Density Functional Theory. *ACS Omega* **2019**, *4*, 3732–3738. [CrossRef] [PubMed]

35. Timsorn, K.; Wongchoosuk, C. Adsorption of NO₂, HCN, HCHO and CO on pristine and amine functionalized boron nitride nanotubes by self-consistent charge density functional tight-binding method. *Mater. Res. Express* **2020**, *7*, 055005. [CrossRef]

36. Mirhaji, E.; Afshar, M.; Rezvani, S.; Yoosefian, M. Boron nitride nanotubes as a nanotransporter for anti-cancer docetaxel drug in water/ethanol solution. *J. Mol. Liq.* **2018**, *271*, 151–156. [CrossRef]

37. García-Toral, D.; Báez, R.M.; Sánchez S, J.I.; Flores-Riveros, A.; Cocoletzi, G.H.; Rivas-Silva, J.F. Encapsulation of Pollutant Gaseous Molecules by Adsorption on Boron Nitride Nanotubes: A Quantum Chemistry Study. *ACS Omega* **2021**, *6*, 14824–14837. [CrossRef]

38. Zhang, X.; Chen, Z.; Chen, D.; Cui, H.; Tang, J. Adsorption behaviour of SO2 and SOF2 gas on Rh-doped BNNT: A DFT study. *Mol. Phys.* **2020**, *118*, e1580394. [CrossRef]

39. Yoosefian, M.; Rahmanifar, E.; Etminan, N. Nanocarrier for levodopa Parkinson therapeutic drug; comprehensive benserazide analysis. *Artif. Cells Nanomed. Biotechnol.* **2018**, *46*, 434–446. [CrossRef]

40. Bououden, W.; Benguerba, Y.; Darwish, A.S.; Attoui, A.; Lemaoui, T.; Balsamo, M.; Erto, A.; Alnashef, I.M. Surface adsorption of Crizotinib on carbon and boron nitride nanotubes as Anti-Cancer drug Carriers: COSMO-RS and DFT molecular insights. *J. Mol. Liq.* **2021**, *338*, 116666. [CrossRef]

41. Yoosefian, M.; Mola, A.; Fooladi, E.; Ahmadzadeh, S. The effect of solvents on formaldehyde adsorption performance on pristine and Pd doped on single-walled carbon nanotube using density functional theory. *J. Mol. Liq.* **2017**, *225*, 34–41. [CrossRef]

42. Cao, M.; Wu, D.; Yoosefian, M.; Sabaei, S.; Jahani, M. Comprehensive study of the encapsulation of Lomustine anticancer drug into single walled carbon nanotubes (SWCNTs): Solvent effects, molecular conformations, electronic properties and intramolecular hydrogen bond strength. *J. Mol. Liq.* **2020**, *320*, 114285. [CrossRef]

43. Yoosefian, M.; Etminan, N. Leucine/Pd-loaded (5,5) single-walled carbon nanotube matrix as a novel nanobiosensors for in silico detection of protein. *Amino Acids* **2018**, *50*, 653–661. [CrossRef]

44. Srihakulung, O.; Maezono, R.; Toochinda, P.; Kongprawechnon, W.; Intarapanich, A.; Lawtrakul, L. Host-Guest Interactions of Plumbagin with β-Cyclodextrin, Dimethyl-β-Cyclodextrin and Hydroxypropyl-β-Cyclodextrin: Semi-Empirical Quantum Mechanical PM6 and PM7 Methods. *Sci. Pharm.* **2018**, *86*, 20. [CrossRef]

45. Stewart, J.J. Optimization of parameters for semiempirical methods VI: More modifications to the NDDO approximations and re-optimization of parameters. *J. Mol. Model.* **2013**, *19*, 1–32. [CrossRef]

46. Archimandritis, A.S.; Papadimitriou, T.; Kormas, K.A.; Laspidou, C.S.; Yannakopoulou, K.; Lazarou, Y.G. Theoretical investigation of microcystin-LR, microcystin-RR and nodularin-R complexation with α-, β-, and γ-cyclodextrin as a starting point for the targeted design of efficient cyanotoxin traps. *Sustain. Chem. Pharm.* **2016**, *3*, 25–32. [CrossRef]

47. Johnson, E.R.; Keinan, S.; Mori-Sánchez, P.; Contreras-García, J.; Cohen, A.J.; Yang, W. Revealing Noncovalent Interactions. *J. Am. Chem. Soc.* **2010**, *132*, 6498–6506. [CrossRef]

48. Contreras-García, J.; Johnson, E.R.; Keinan, S.; Chaudret, R.; Piquemal, J.-P.; Beratan, D.N.; Yang, W. NCIPLOT: A Program for Plotting Noncovalent Interaction Regions. *J. Chem. Theory Comput.* **2011**, *7*, 625–632. [CrossRef]

49. Braga, L.S.; Leal, D.H.; Kuca, K.; Ramalho, T.C. Perspectives on the Role of the Frontier Effective-for-Reaction Molecular Orbital (FERMO) in the Study of Chemical Reactivity: An Updated Review. *Curr. Org. Chem.* **2020**, *24*, 314–331. [CrossRef]

50. Park, J.H.; Nah, T.H. Binding forces contributing to the complexation of organic molecules with β-cyclodextrin in aqueous solution. *J. Chem. Soc. Perkin Trans. 2* **1994**, *6*, 1359–1362. [CrossRef]

51. Liu, L.; Guo, Q.-X. Novel Prediction for the Driving Force and Guest Orientation in the Complexation of α- and β-Cyclodextrin with Benzene Derivatives. *J. Phys. Chem. B* **1999**, *103*, 3461–3467. [CrossRef]

52. Liu, C.; Zhao, H.; Hou, P.; Qian, B.; Wang, X.; Guo, C.; Wang, L. Efficient Graphene/Cyclodextrin-Based Nanocontainer: Synthesis and Host–Guest Inclusion for Self-Healing Anticorrosion Application. *ACS Appl. Mater. Interfaces* **2018**, *10*, 36229–36239. [CrossRef] [PubMed]

53. Fu, L. Cyclodextrin Functionalized Graphene and Its Applications. In *Graphene Functionalization Strategies: From Synthesis to Applications*; Khan, A., Jawaid, M., Neppolian, B., Asiri, A.M., Eds.; Springer: Singapore, 2019; pp. 193–213.

54. Shao, D.; Sheng, G.; Chen, C.; Wang, X.; Nagatsu, M. Removal of polychlorinated biphenyls from aqueous solutions using β-cyclodextrin grafted multiwalled carbon nanotubes. *Chemosphere* **2010**, *79*, 679–685. [CrossRef]

55. Tan, P.; Hu, Y. Improved synthesis of graphene/β-cyclodextrin composite for highly efficient dye adsorption and removal. *J. Mol. Liq.* **2017**, *242*, 181–189. [CrossRef]

56. Fraga, T.M.; Carvalho, M.; Ghislandi, M.; Sobrinho, M.A.M. Functionalized Graphene-Based Materials as Innovative Adsorbents of Organic Pollutants: A Concise Overview. *Braz. J. Chem. Eng.* **2019**, *36*, 1–31. [CrossRef]

57. Yu, S.; Wang, X.; Pang, H.; Zhang, R.; Song, W.; Fu, D.; Hayat, T.; Wang, X. Boron nitride-based materials for the removal of pollutants from aqueous solutions: A review. *Chem. Eng. J.* **2018**, *333*, 343–360. [CrossRef]

58. Wang, Y.; Tang, W.; Peng, Y.; Chen, Z.; Chen, J.; Xiao, Z.; Zhao, X.; Qu, Y.; Li, J. Predicting the adsorption of organic pollutants on boron nitride nanosheets via in silico techniques: DFT computations and QSAR modeling. *Environ. Sci. Nano* **2021**, *8*, 795–805. [CrossRef]

59. Huang, Q.; Chai, K.; Zhou, L.; Ji, H. A phenyl-rich β-cyclodextrin porous crosslinked polymer for efficient removal of aromatic pollutants: Insight into adsorption performance and mechanism. *Chem. Eng. J.* **2020**, *387*, 124020. [CrossRef]

60. Chen, X.; Jia, S.; Ding, N.; Shi, J.; Wang, Z. Capture of aromatic organic pollutants by hexagonal boron nitride nanosheets: Density functional theoretical and molecular dynamic investigation. *Environ. Sci. Nano* **2016**, *3*, 1493–1503. [CrossRef]

61. Guo, Y.; Guo, S.; Ren, J.; Zhai, Y.; Dong, S.; Wang, E. Cyclodextrin Functionalized Graphene Nanosheets with High Supramolecular Recognition Capability: Synthesis and Host−Guest Inclusion for Enhanced Electrochemical Performance. *ACS Nano* **2010**, *4*, 4001–4010. [CrossRef]

62. Gao, Y.-S.; Wu, L.-P.; Zhang, K.-X.; Xu, J.-K.; Lu, L.-M.; Zhu, X.-F.; Wu, Y. Electroanalytical method for determination of shikonin based on the enhancement effect of cyclodextrin functionalized carbon nanotubes. *Chin. Chem. Lett.* **2015**, *26*, 613–618. [CrossRef]

63. Jaiyong, P.; Bryce, R.A. Approximate quantum chemical methods for modelling carbohydrate conformation and aromatic interactions: β-cyclodextrin and its adsorption on a single-layer graphene sheet. *Phys. Chem. Chem. Phys.* **2017**, *19*, 15346–15355. [CrossRef] [PubMed]